2024 European Control Conference (ECC)
June 25-28, 2024. Stockholm, Sweden

Interval Observer Design for an Uncertain Time-Varying Quasi-Linear System Model of Lithium-Ion Batteries

Marit Lahme[1], Andreas Rauh[1] and Guillaume Defresne[2]

Abstract— **Lithium-ion batteries are currently used in numerous applications, for example in electric vehicles and energy storage systems. Accurately estimating the dynamic behavior is crucial to safely and efficiently charge and discharge the battery cells. This can be done with the help of stochastic or interval based identification routines which require an accurate state estimation. In previous works, we used an interval observer based on a Luenberger observer structure to estimate the lower and upper bounds of the state variables. However, with this approach it was necessary to use specified input current profiles to charge or discharge the battery cells, otherwise, the estimation uncertainty increased over time. In this paper, we aim to estimate the state variables during system operation without using specified input current profiles. A promising approach is a TNL observer, which was introduced for uncertain time-invariant systems in the literature, that provides multiple design degrees of freedom. The TNL observer is extended to an uncertain time-varying system model of lithium-ion batteries in this work. The time-varying part is herein considered with two different approaches. At first, a nominal system model is considered where the time-varying part is treated as a measurement uncertainty and secondly it is considered using a polytopic representation of the system matrix. The TNL observer was successfully extended to the time-varying system model of a lithium-ion battery. The polytopic representation of the system matrix leads to more accurate estimation results in comparison to the nominal approach.**

I. INTRODUCTION

Nowadays, lithium-ion batteries are used in a wide range of applications. They are commonly used in consumer electronics but their usage is getting popular in recent years in mobility applications for energy storage systems in electric or hybrid vehicles. Moreover, they are employed in renewable energy systems as large-scale energy storage solutions in electric power grids. For a safe and efficient operation of these battery systems, it is necessary to consider the dynamic behavior of the individual battery cells to avoid overcharging and low discharging, which can lead to irreversible degradation. The information about the dynamic behavior can also be used to detect reversible and irreversible aging effects. In the worst case, those aging and degradation effects can result in a failure of the battery cell and in a thermal runaway. In control oriented applications, like battery management systems, equivalent circuit models are typically used to model and predict the dynamic behavior of lithium-ion batteries. However, measuring the state variables is often not possible or economically feasible, because they are either not directly measurable or the costs would be too high. Furthermore, the estimation of the dynamic behavior is subject to process and measurement noise and parametric uncertainty. Therefore, we make use of interval observers to estimate lower and upper bounds of the state variables with respect to the uncertainties mentioned above, so that these bounds always enclose the true value. Those observers are widely used for the state estimation of uncertain dynamic systems [1]. In previous work, we used an interval observer design based on a Luenberger observer structure [2]. The drawback of this approach is, that the estimation uncertainty may increase over time which makes it necessary to use specified input current profiles to charge or discharge the battery cell during the estimation process. We aim to estimate the state variables during system operation without using specified input current profiles. Investigating other design approaches is therefore necessary. A promising approach is an interval observer design that we will call TNL observer throughout this paper, which was introduced by Z. Wang et al. for uncertain time-invariant discrete-time linear systems [3]. This interval observer design provides two additional design parameters $\mathbf{T}$ and $\mathbf{N}$ besides the observer gain matrix $\mathbf{L}$. It also allows including an H_∞ technique to reduce the influence of uncertainties on the estimation result. In this paper, the parameterization of the TNL observer is obtained by solving a set of LMIs. The TNL design approach has already been used for continuous-time and discrete-time linear parameter-varying systems [4]–[7], linear time-varying systems [8], [9] and switched systems [10]. This type of observer structure is typically combined with zonotope and ellipsoid techniques to enclose uncertainties. Instead of using zonotope or ellipsoid enclosing techniques, we focus on uncertainty models that require low computational effort, because this state estimation will be the basis for a computational procedure that identifies the open-circuit voltage characteristic of a lithium-ion battery during system operation. We therefore analyze two approaches to design a TNL observer for an uncertain time-varying quasi-linear system model of a lithium-ion battery. At first, a nominal system model is considered, where the system is divided into a time-invariant and a time-varying part. The time-varying part is herein assumed to be mapped onto the process and measurement uncertainty. This simplifies solving the LMIs. Secondly, a system model with a polytopic representation of the system matrix is investigated to consider the time-varying part. Within the nominal system approach, a cascaded ob-

[1]Carl von Ossietzky Universität Oldenburg, Department of Computing Science, Group: Distributed Control in Interconnected Systems, D-26111 Oldenburg, Germany, {marit.lahme, andreas.rauh}@uni-oldenburg.de
[2]Institut Supérieur de l'Aéronautique et de l'Espace (ISAE-SUPAERO), F-31055 Toulouse, France guillaume.defresne@student.isae-supaero.fr

server structure is used to enhance the estimation accuracy. In the literature, a cascaded observer structure is typically implemented by dividing a particular part of a dynamical system model into corresponding subsystems to either reduce the complexity of the considered dynamical system model, to reduce the influence of noise on the estimation result, or to estimate the state vector of a dynamical system with time-delays in the output [11]–[14]. In [15] and [16], a cascaded observer design is used to enhance the estimation result. In the former case, the authors at first designed a least squares filter to roughly estimate an auxiliary state vector of a linear time-varying system and afterwards used a high-order sliding-mode observer in combination with an error compensation equation to accurately reconstruct the state vector of the system. In the latter case, the authors designed two observers in order to estimate the position of a sensorless permanent magnet synchronous motor. Here, the first observer provides an estimate for the back-EMF which is used in the second observer to accurately estimate the position of the motor. In this paper, we will design two cascaded observers in combination with a contractor approach to accurately estimate the state vector of a dynamical system. In contrast to the literature mentioned above, we exploit an accurate estimation result of a specific state variable of the first observer to enhance the estimation accuracy of all state variables with the second observer.

This paper is structured as follows. Sec. II summarizes the modeling of lithium-ion batteries and shows how observability is guaranteed for the corresponding state-space system by augmenting the measurement vector. The general structure of a TNL observer and parameterization details are presented in Sec. III-A. Subsequently, TNL observers are designed for a nominal system model and a system model with a polytopic representation of the system matrix in Secs. III-B and III-C. Simulation results are further presented in this section. Implementation details are given in Sec. IV. The paper is concluded with a brief summary and an outlook on future work in Sec. V.

Notation. Matrices and vectors are denoted by capitalized bold letters and lowercase bold letters, respectively. A vector $\mathbf{m}$ *is meant to be a column vector. Row vectors are denoted by the transposed form* $\mathbf{m}^{\mathrm{T}}$. *The operators* $\geq,\ >,\ \leq,\ <$ *as well as the lower and upper bounds of a matrix* $\mathbf{M}$, *denoted by* $\underline{\mathbf{M}}$ *and* $\overline{\mathbf{M}}$, *are employed in an elementwise form.* $\mathbf{M}^{+}$ *and* $\mathbf{M}^{-}$ *for a matrix* $\mathbf{M}$ *are defined by* $\mathbf{M}^{+} = \max\{\mathbf{0}, \mathbf{M}\}$ *and* $\mathbf{M}^{-} = \mathbf{M}^{+} - \mathbf{M}$. *The* $n \times n$ *identity matrix is denoted by* $\mathbf{I}_n$. *The* L_2*-norm is represented by* $\| \, \|_2$. $\mathbf{M} \succ 0$ $(\prec 0)$ *denotes a positive (negative) definite matrix. An asterisk * is used to indicate terms that are induced by symmetry.*

II. MODELING OF LITHIUM-ION BATTERIES

Equivalent circuit models are often used in control oriented applications to model the dynamic behavior of lithium-ion batteries. In this paper, an equivalent circuit model consisting of a series resistance, two RC sub-networks, a state dependent voltage source representing the open-circuit voltage and a voltage source denoting the disturbance voltage, which represents a systematic model mismatch as shown in Fig. 1, is used to represent the dynamic behavior. The disturbance voltage represents deviations between the model and the system and therefore comprises all effects that are not directly modelled with this equivalent circuit model. The terminal current i_{T} is used as an input to charge or discharge the battery cell and the terminal voltage v_{T} is measured. The measurement is subject to measurement uncertainty, which is assumed to be unknown but bounded. In Fig. 1, the two RC sub-networks represent dynamic processes with short (τ_{TS}) and large (τ_{TL}) time constants, resulting from, for example, polarization effects and diffusion processes. The series resistance R_{S} causes an instantaneous voltage drop of the terminal voltage, after a load is connected to the battery. The open-circuit voltage v_{OC} depends on the state of charge (SOC) $\sigma(t)$. The system parameters vary due to numerous influence factors such as aging effects and temperature dependencies.

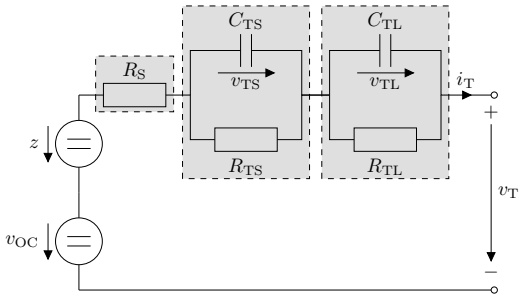

Fig. 1. Equivalent circuit model of a lithium-ion battery including a disturbance voltage $z(t)$.

With the state vector

$$\mathbf{x}(t) = \begin{bmatrix} \sigma(t) & v_{\mathrm{TS}}(t) & v_{\mathrm{TL}}(t) & z(t) \end{bmatrix}^{T} \ , \tag{1}$$

a quasi-linear system model corresponding to

$$\begin{aligned} \dot{\mathbf{x}}(t) &= \mathbf{A}\left(\sigma(t)\right) \cdot \mathbf{x}(t) + \mathbf{b}\left(\sigma(t)\right) \cdot i_{\mathrm{T}}(t) \ , \\ \mathrm{y}^{*}(t) &= \mathrm{y}(t) - \mathrm{d}\left(\sigma(t)\right) \cdot i_{\mathrm{T}}(t) \ , \\ &= \mathbf{c}^{T}\left(\sigma(t)\right) \cdot \mathbf{x}(t) + v(t) \ , \end{aligned} \tag{2}$$

can be obtained with the state vector $\mathbf{x} \in \mathbb{R}^n$, the measurement $\mathrm{y} \in \mathbb{R}^m$, the input current $i_{\mathrm{T}} \in \mathbb{R}^p$, the measurement uncertainty $v \in \mathbb{R}^m$ and the SOC $\sigma(t) \in [0\,;\,1]$. The matrices and vectors $\mathbf{A}$, $\mathbf{b}$, $\mathbf{c}^T$, and d are of appropriate dimensions. The output equation is based on Kirchhoff's voltage law, so that the equation

$$\begin{aligned} \mathrm{y}(t) &= v_{\mathrm{T}}(t) + v(t) \\ &= v_{\mathrm{OC}}(\sigma(t)) - v_{\mathrm{TS}}(t) - v_{\mathrm{TL}}(t) + z(t) \\ &\quad - i_{\mathrm{T}}(t) \cdot R_{\mathrm{S}}\left(\sigma(t)\right) + v(t) \end{aligned} \tag{3}$$

holds. The state dependent system parameters $R_{\iota}(\sigma(t))$ with $\iota \in \{\mathrm{S}, \mathrm{TS}, \mathrm{TL}\}$ and $C_{\iota}(\sigma(t))$ with $\iota \in \{\mathrm{TS}, \mathrm{TL}\}$ as well as the open-circuit voltage $v_{\mathrm{OC}}(\sigma(t))$ are nonlinear functions of the SOC. The disturbance voltage $z(t)$ is assumed to be represented by an integrator disturbance model

$$\dot{z}(t) = 0 \ . \tag{4}$$

With (1) and (3), the matrices and vectors $\mathbf{A}$, $\mathbf{b}$, $\mathbf{c}^T$, and d for the equivalent circuit model of a lithium-ion battery shown in Fig. 1 are defined as

$$\mathbf{A}\left(\sigma(t)\right) = \begin{bmatrix} 0 & 0 & 0 & 0 \\ 0 & \frac{-1}{\tau_{\mathrm{TS}}(\sigma(t))} & 0 & 0 \\ 0 & 0 & \frac{-1}{\tau_{\mathrm{TL}}(\sigma(t))} & 0 \\ 0 & 0 & 0 & 0 \end{bmatrix} , \tag{5}$$

$$\mathbf{b}\left(\sigma(t)\right) = \begin{bmatrix} \frac{-1}{C_{\mathrm{Bat}}} & \frac{1}{C_{\mathrm{TS}}(\sigma(t))} & \frac{1}{C_{\mathrm{TL}}(\sigma(t))} & 0 \end{bmatrix}^T , \tag{6}$$

$$\mathbf{c}^T\left(\sigma(t)\right) = \begin{bmatrix} \eta_{\mathrm{OC}}\left(\sigma(t)\right) & -1 & -1 & 1 \end{bmatrix} , \tag{7}$$

$$\mathrm{d}\left(\sigma(t)\right) = -R_{\mathrm{S}}(\sigma(t)) \tag{8}$$

with $\tau_\iota(\sigma(t)) = C_\iota(\sigma(t)) \cdot R_\iota(\sigma(t))$, $\iota \in \{\mathrm{TS}, \mathrm{TL}\}$. Here, $\eta_{\mathrm{OC}}\left(\sigma(t)\right)$ can be a linear or nonlinear function of $\sigma(t)$ with $\eta_{\mathrm{OC}}\left(\sigma(t)\right) \cdot \sigma(t) = v_{\mathrm{OC}}(\sigma(t))$. The first row in the state equation describes the integrating behavior between the terminal current i_{T} and the SOC with respect to the nominal capacitance C_{Bat} of the battery cell. The open-circuit voltage characteristic is chosen to be approximated with

$$v_{\mathrm{OC}}(\sigma(t)) = v_0 \cdot e^{v_1 \cdot \sigma(t)} + \sum_{i=0}^{3} v_{i+2} \cdot \sigma^i(t) \ , \tag{9}$$

which can be rewritten in the quasi-linear form [2]

$$\begin{aligned} \tilde{v}_{\mathrm{OC}}(\sigma(t)) &= v_{\mathrm{OC}}(\sigma(t)) - v_0 - v_2 \\ &= \eta_{\mathrm{OC}}\left(\sigma(t)\right) \cdot \sigma(t) \end{aligned} \tag{10}$$

with

$$\eta_{\mathrm{OC}}\left(\sigma(t)\right) = \left(v_0 \frac{e^{v_1 \sigma(t)} - 1}{\sigma(t)} + v_3 + v_4 \sigma(t) + v_5 \sigma^2(t) \right) . \tag{11}$$

This quasi-linear representation of the open-circuit voltage is used in the system model (2) with the output vector defined in (7).

To implement the TNL observer, the system is temporally discretized with a constant step size T_{d} and with the help of the explicit Euler method. This is sufficiently accurate, because the sampling time is much smaller than the time constants of the observer dynamics and the discretization errors are therefore assumed to be included in the process and measurement uncertainty. The exact values $\mathbf{x}(t_k)$ are approximated by $\mathbf{x}_k$, so that the discretized system can be written as

$$\begin{aligned} \mathbf{x}_{k+1} &= \mathbf{A}_{\mathrm{d}}(\sigma_k) \cdot \mathbf{x}_k + \mathbf{b}_{\mathrm{d}}(\sigma_k) \cdot i_{\mathrm{T},k} \ , \\ \mathrm{y}_k^* &= \mathbf{c}^T(\sigma_k) \cdot \mathbf{x}_k \ , \\ \mathbf{A}_{\mathrm{d}}(\sigma_k) &= \mathbf{I}_n + T_{\mathrm{d}} \cdot \mathbf{A}(\sigma_k) \ , \\ \mathbf{b}_{\mathrm{d}}(\sigma_k) \cdot i_{\mathrm{T},k} &= T_{\mathrm{d}} \cdot \mathbf{b}(\sigma_{\mathbf{k}}) \cdot i_{\mathrm{T},k} \ . \end{aligned} \tag{12}$$

With the system matrix $\mathbf{A}\left(\sigma(t)\right)$ and the output matrix $\mathbf{c}^T\left(\sigma(t)\right)$ alone, given in (5) and (7), the continuous-time system (2) is not observable, when treated as linear parameter-varying. Thus, the output matrix is augmented by a second measurement. We choose the first derivative of the terminal voltage

$$\mathbf{y}(t) = \begin{bmatrix} v_{\mathrm{T}}(t) \\ \dot{v}_{\mathrm{T}}(t) \end{bmatrix} \in \mathbb{R}^m \ , \ m = 2 \tag{13}$$

as a second measurement. The first derivative of the terminal voltage $\dot{v}_{\mathrm{T}}(t)$ can not be measured directly, so that it has to be approximated. With the help of the Taylor expansion, the terminal voltage $v_{\mathrm{T}}(t)$ can be approximated by

$$\begin{aligned} v_{\mathrm{T},k+1} &= h(\mathbf{x}_{k+1}) \\ &= h(\mathbf{x}_k) + \left.\frac{\partial h}{\partial \mathbf{x}}\right|_{\mathbf{x}=\mathbf{x}_k} (\mathbf{x}_{k+1} - \mathbf{x}_k) + r_{\mathrm{l},k+1} \\ &= v_{\mathrm{T},k} + \tilde{\mathbf{c}}^T \cdot (\mathbf{A}_{\mathrm{d},k} \cdot \mathbf{x}_k + \mathbf{b}_{\mathrm{d},k} \cdot i_{\mathrm{T},k} - \mathbf{x}_k) + r_{\mathrm{l},k+1} \end{aligned} \tag{14}$$

with $\tilde{\mathbf{c}}^T \in \left[\tilde{\mathbf{c}}^T\right]\left([\sigma_k]\right)$ and $r_{\mathrm{l},k+1} \in [r_{\mathrm{l},k+1}]$ denoting the linearization error. Based on (14), the first derivative of the terminal voltage can be approximated as

$$\begin{aligned} \Delta T \cdot \dot{v}_{\mathrm{T},k} &= \Delta T \cdot \left(\tfrac{v_{\mathrm{T},k+1} - v_{\mathrm{T},k}}{\Delta T} + r_{\mathrm{d},k} \right) \\ &= \tilde{\mathbf{c}}^T \cdot (\mathbf{A}_{\mathrm{d},k} \cdot \mathbf{x}_k + \mathbf{b}_{\mathrm{d},k} \cdot i_{\mathrm{T},k} - \mathbf{x}_k) + r_k \end{aligned} \tag{15}$$

with the discretization error $r_{\mathrm{d},k}$ and the approximation error

$$r_k \in [r_k] = [r_{\mathrm{l},k+1}] + \Delta T \cdot [r_{\mathrm{d},k}] \ . \tag{16}$$

The time-increment ΔT is defined as the time difference between the discretization steps k and $k+1$ and is therefore equal to the discretization step size T_{d}. Taking into account (1), (2), (5)-(8), and (15), the output equation of the augmented discretized system can be written as

$$\begin{aligned} \mathbf{y}_k^* &=: h_1(v_{\mathrm{T},k},\ v_{\mathrm{T},k+1},\ i_{\mathrm{T},k},\ \mathbf{x}_k) \\ &= \begin{bmatrix} v_{\mathrm{T},k} + i_{\mathrm{T},k} \cdot R_{\mathrm{S}}(\sigma_k) + v_k \\ \frac{v_{\mathrm{T},k+1} - v_{\mathrm{T},k}}{\Delta T} + r_{\mathrm{d},k} - \frac{1}{\Delta T}\left(\tilde{\mathbf{c}}^T \left(\mathbf{b}_{\mathrm{d},k} i_{\mathrm{T},k} - \mathbf{x}_k\right) + r_k\right) \end{bmatrix} \\ &= \begin{bmatrix} \mathbf{c}^T\left(\sigma_k\right) \cdot \mathbf{x}_k + v_k \\ \frac{1}{\Delta T}\left(\tilde{\mathbf{c}}^T \cdot \mathbf{A}_{\mathrm{d},k} \cdot \mathbf{x}_k\right) \end{bmatrix} \ . \end{aligned} \tag{17}$$

Considering (10) and (17), we define the augmented output matrix of the discretized system as

$$\mathbf{C}\left(\sigma_k\right) = \begin{bmatrix} \eta_{\mathrm{OC}}\left(\sigma_k\right) & -1 & -1 & 1 \\ \frac{1}{\Delta T} \frac{\partial \tilde{v}_{\mathrm{OC}}}{\partial \sigma}\big|_{\sigma=\sigma_k} & -\frac{\mathrm{A}_{\mathrm{d},22}(\sigma_k)}{\Delta T} & -\frac{\mathrm{A}_{\mathrm{d},33}(\sigma_k)}{\Delta T} & \frac{1}{\Delta T} \end{bmatrix} . \tag{18}$$

Remark. Note that the nonlinear system model is observable, cf. [17]. This also applies to a simplified model, which does not include the disturbance voltage $z(t)$. Hence, augmenting the measurement vector is only necessary for the quasi-linear system model, that includes the disturbance voltage.

III. INTERVAL OBSERVER DESIGN

In this section, the general structure of the TNL observer is introduced for a general state-space model subject to process and measurement noise. Afterwards, the TNL observer is extended to an uncertain time-varying system. At first, a TNL observer is designed for a nominal system model, where the time-varying part is treated as a process and measurement uncertainty and, secondly, the time-varying part is considered using a polytopic representation of the system matrix.

A. General Structure of the TNL Observer

The TNL observer proposed by Z. Wang et al. in [3] was originally introduced for an uncertain time-invariant system corresponding to

$$\begin{aligned} \mathbf{x}_{k+1} &= \mathbf{A}_\mathrm{d} \cdot \mathbf{x}_k + \mathbf{B}_\mathrm{d} \cdot \mathbf{u}_k + \mathbf{E}_\mathrm{d} \cdot \boldsymbol{w}_k \\ \mathbf{y}_k &= \mathbf{C} \cdot \mathbf{x}_k + \boldsymbol{v}_k \end{aligned} \tag{19}$$

with the state vector $\mathbf{x}_k \in \mathbb{R}^n$, the measurement $\mathbf{y}_k \in \mathbb{R}^m$, the input $\mathbf{u}_k \in \mathbb{R}^p$, the process uncertainty $\boldsymbol{w}_k \in \mathbb{R}^q$ and the measurement uncertainty $\boldsymbol{v}_k \in \mathbb{R}^m$. $\mathbf{A}_\mathrm{d}$, $\mathbf{B}_\mathrm{d}$, $\mathbf{C}$, and $\mathbf{E}_\mathrm{d}$ are constant matrices of appropriate dimensions. The process and measurement uncertainties are assumed to be bounded and symmetric, so that $\underline{\boldsymbol{w}}_k \leq \boldsymbol{w}_k \leq \overline{\boldsymbol{w}}_k$ and $\underline{\boldsymbol{v}}_k \leq \boldsymbol{v}_k \leq \overline{\boldsymbol{v}}_k$. The TNL observer for system (19) is defined as

$$\begin{aligned} \overline{\zeta}_{k+1} &= \mathbf{T}\mathbf{A}_\mathrm{d}\hat{\overline{\mathbf{x}}}_k + \mathbf{T}\mathbf{B}_\mathrm{d}\mathbf{u}_k + \mathbf{L}(\mathbf{y}_k - \mathbf{C}\hat{\overline{\mathbf{x}}}_k) + \overline{\boldsymbol{\Delta}}_k \ , \\ \hat{\overline{\mathbf{x}}}_k &= \overline{\zeta}_k + \mathbf{N}\mathbf{y}_k \ , \\ \underline{\zeta}_{k+1} &= \mathbf{T}\mathbf{A}_\mathrm{d}\hat{\underline{\mathbf{x}}}_k + \mathbf{T}\mathbf{B}_\mathrm{d}\mathbf{u}_k + \mathbf{L}(\mathbf{y}_k - \mathbf{C}\hat{\underline{\mathbf{x}}}_k) + \underline{\boldsymbol{\Delta}}_k \ , \\ \hat{\underline{\mathbf{x}}}_k &= \underline{\zeta}_k + \mathbf{N}\mathbf{y}_k \ , \end{aligned} \tag{20}$$

with $\overline{\zeta}_k \in \mathbb{R}^n$ and $\underline{\zeta}_k \in \mathbb{R}^n$ as intermediate variables and $\overline{\boldsymbol{\Delta}}_k$ and $\underline{\boldsymbol{\Delta}}_k$ given as

$$\begin{aligned} \overline{\boldsymbol{\Delta}}_k =& (\mathbf{T}\mathbf{E}_\mathrm{d})^+ \overline{\boldsymbol{w}}_k - (\mathbf{T}\mathbf{E}_\mathrm{d})^- \underline{\boldsymbol{w}}_k + \mathbf{L}^+ \overline{\boldsymbol{v}}_k - \mathbf{L}^- \underline{\boldsymbol{v}}_k \\ &+ \mathbf{N}^+ \overline{\boldsymbol{v}}_{k+1} - \mathbf{N}^- \underline{\boldsymbol{v}}_{k+1} \ , \\ \underline{\boldsymbol{\Delta}}_k =& (\mathbf{T}\mathbf{E}_\mathrm{d})^+ \underline{\boldsymbol{w}}_k - (\mathbf{T}\mathbf{E}_\mathrm{d})^- \overline{\boldsymbol{w}}_k + \mathbf{L}^+ \underline{\boldsymbol{v}}_k - \mathbf{L}^- \overline{\boldsymbol{v}}_k \\ &+ \mathbf{N}^+ \underline{\boldsymbol{v}}_{k+1} - \mathbf{N}^- \overline{\boldsymbol{v}}_{k+1} \ . \end{aligned} \tag{21}$$

The structure of this interval observer is shown in Fig. 2. If $\mathbf{T} = \mathbf{I}_n$ and $\mathbf{N} = \mathbf{0}$, the TNL observer has a Luenberger observer structure.

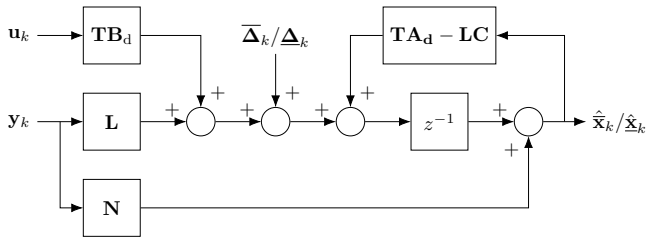

Fig. 2. General structure of the TNL observer (cf. [3]).

To guarantee stable error dynamics and to reliably bound the true value with lower and upper bounds, so that $\hat{\underline{\mathbf{x}}}_k \leq \mathbf{x}_k \leq \hat{\overline{\mathbf{x}}}_k$, the matrix $(\mathbf{T}\mathbf{A}_\mathrm{d} - \mathbf{L}\mathbf{C})$ has to be Schur stable and elementwise non-negative. Furthermore, the initial estimated state vector has to be chosen, so that $\hat{\underline{\mathbf{x}}}_0 \leq \mathbf{x}_0 \leq \hat{\overline{\mathbf{x}}}_0$. In summary, the following conditions have to be fulfilled

$$\begin{aligned} &\hat{\underline{\mathbf{x}}}_0 \leq \mathbf{x}_0 \leq \hat{\overline{\mathbf{x}}}_0 \\ &\mathbf{T} + \mathbf{N}\mathbf{C} = \mathbf{I}_n \\ &(\mathbf{T}\mathbf{A}_\mathrm{d} - \mathbf{L}\mathbf{C}) \geq 0 \\ &|\lambda_\iota(\mathbf{T}\mathbf{A}_\mathrm{d} - \mathbf{L}\mathbf{C})| < 1 \ , \ \iota = 1, \ \dots \ , n \ . \end{aligned} \tag{22}$$

The conditions (22) are formulated as a set of matrix inequalities, to be able to compute the design parameters $\mathbf{T}$, $\mathbf{N}$, and $\mathbf{L}$ of the TNL observer. We obtain

$$\begin{aligned} &\mathbf{T} = \mathbf{I}_n - \mathbf{N}\mathbf{C} \\ &(\mathbf{T}\mathbf{A}_\mathrm{d} - \mathbf{L}\mathbf{C}) \geq 0 \\ &(\mathbf{T}\mathbf{A}_\mathrm{d} - \mathbf{L}\mathbf{C})^T \mathbf{P} (\mathbf{T}\mathbf{A}_\mathrm{d} - \mathbf{L}\mathbf{C}) - \mathbf{P} \prec 0 \\ &\mathbf{P} \succ 0 \ , \end{aligned} \tag{23}$$

with an arbitrary diagonal matrix $\mathbf{P} \in \mathbb{R}^n$, given that $\hat{\underline{\mathbf{x}}}_0 \leq \mathbf{x}_0 \leq \hat{\overline{\mathbf{x}}}_0$. To ensure, that the lower and upper bounds are as close to the true value as possible, an H_∞ technique can be included in the design process, so that $\| \ \overline{\mathbf{e}} \ \|_2 < \gamma \ \| \ \overline{\mathbf{d}}_k \ \|_2$, with $\overline{\mathbf{e}} = \hat{\overline{\mathbf{x}}}_k - \mathbf{x}_k$, $\overline{\mathbf{d}}_k = \begin{bmatrix} \overline{\Delta}_k - \mathbf{T}\mathbf{E}_\mathrm{d}\boldsymbol{w}_k & \boldsymbol{v}_k & \boldsymbol{v}_{k+1} \end{bmatrix}^T$ and a given scalar γ (analogously for the lower bound). Then, the following conditions have to be fulfilled [3]

$$\begin{aligned} &\begin{bmatrix} -\mathbf{P} + \mathbf{I}_n & * & * & * & * \\ 0 & -\gamma^2 \mathbf{I}_n & * & * & * \\ 0 & 0 & -\gamma^2 \mathbf{I}_m & * & * \\ 0 & 0 & 0 & -\gamma^2 \mathbf{I}_m & * \\ \mathbf{P}\mathbf{M} & \mathbf{P} & \mathbf{P}\mathbf{L} & \mathbf{P}\mathbf{N} & -\mathbf{P} \end{bmatrix} \prec 0 \ , \\ &\mathbf{M} = (\mathbf{T}\mathbf{A}_\mathrm{d} - \mathbf{L}\mathbf{C}) \ , \\ &\mathbf{P} = \mathrm{diag}(p_{11}, \dots, p_{nn}) \ , \\ &\mathbf{P} \succ 0 \ , \\ &\mathbf{P}\mathbf{M} \geq 0 \ , \\ &\gamma > 0 \ . \end{aligned} \tag{24}$$

Note that the inequalities (24) are nonlinear due to the multiplicative couplings $\mathbf{PM}$, $\mathbf{PL}$, and $\mathbf{PN}$. As shown in [3], (24) can be written as a set of LMIs by applying a linearizing variable substitution.

B. Nominal System Model

To design a TNL observer for a time-varying system, the system (2) is at first split into a time-invariant and a time-varying part. We therefore obtain a state-space model corresponding to

$$\begin{aligned} \mathbf{x}_{k+1} &= \mathbf{A}_\mathrm{d}(\sigma_\mathrm{f}) \cdot \mathbf{x}_k + \mathbf{b}_\mathrm{d}(\sigma_\mathrm{f}) \cdot i_{\mathrm{T},k} + \mathbf{E}_\mathrm{d} \cdot \boldsymbol{w}_k \ , \\ \mathbf{y}_k^* &= \mathbf{C}(\sigma_\mathrm{f}) \cdot \mathbf{x}_k + \boldsymbol{v}_k \ . \end{aligned} \tag{25}$$

The time-varying part is herein assumed to be part of the process and measurement noise. The matrices and vectors $\mathbf{A}_\mathrm{d}, \mathbf{b}_\mathrm{d}$, and $\mathbf{C}$ are evaluated for a chosen constant value σ_f for the SOC. The estimated state variables obtained with this approach are shown in Fig. 3. The system is simulated for an input current corresponding to Fig. 4. For details about the implementation, the reader is referred to Sec. IV. In Fig. 3, it is obvious that the state of charge is closely bounded, but the lower and upper bounds for the other state variables are very conservative and are not applicable for the identification of the dynamic behavior. We introduce a cascaded observer structure shown in Fig. 5, that makes use of the accurate estimation of the state of charge to also closely bound the other state variables. Therefore, the second interval observer is provided with a virtual measurement

$$\begin{aligned} \mathbf{y}_{2,k+1}^* &=: h_2(v_{\mathrm{T},k+1}, \ i_{\mathrm{T},k+1}, \ \mathbf{x}_{k+1}) \\ &= \begin{bmatrix} v_{\mathrm{T},k+1} + i_{\mathrm{T},k+1} \cdot R_\mathrm{S}(\sigma_{k+1}) \\ \frac{1}{2}\left(\hat{\underline{\sigma}}_{k+1} + \hat{\overline{\sigma}}_{k+1}\right) \end{bmatrix} + \boldsymbol{v}_{2,k+1} \ , \end{aligned} \tag{26}$$

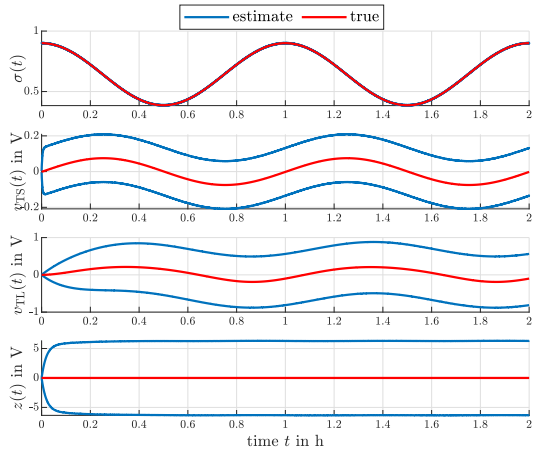

Fig. 3. Estimation results obtained with the nominal system model.

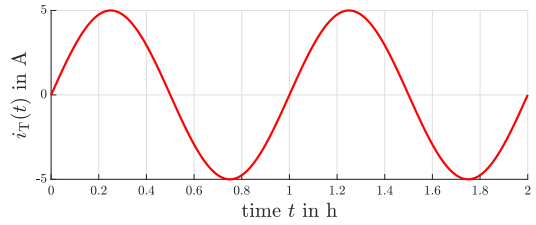

Fig. 4. Input current $i_{\mathrm{T}}(t)$.

consisting of the true measurement of the terminal voltage and the estimated state of charge from the first interval observer. The measurement uncertainty $\boldsymbol{v}_{2,k+1}$ is computed as

$$\boldsymbol{v}_{2,k+1} = \begin{bmatrix} v_{k+1} \\ \hat{\overline{\sigma}}_{k+1} - \frac{1}{2}\left(\hat{\underline{\sigma}}_{k+1} + \hat{\overline{\sigma}}_{k+1}\right) \end{bmatrix} \tag{27}$$

for the estimation of the upper bound and

$$\boldsymbol{v}_{2,k+1} = \begin{bmatrix} v_{k+1} \\ \hat{\underline{\sigma}}_{k+1} - \frac{1}{2}\left(\hat{\underline{\sigma}}_{k+1} + \hat{\overline{\sigma}}_{k+1}\right) \end{bmatrix} \tag{28}$$

for the estimation of the lower bound, where v_{k+1} is the first row of the measurement uncertainty $\boldsymbol{v}_{k+1}$ and corresponds to the measurement uncertainty $v(t)$ in (3). According to (26), the output matrix of the second observer can be written as

$$\mathbf{C}_2\left(\sigma_{\mathrm{f}}\right) = \begin{bmatrix} \eta_{\mathrm{OC}}\left(\sigma_{\mathrm{f}}\right) & -1 & -1 & 1 \\ 1 & 0 & 0 & 0 \end{bmatrix} . \tag{29}$$

Both TNL observers of the cascaded structure estimate the state vector with lower and upper bounds at the same time step, so that the true value is always enclosed. Therefore, the true value is included in the estimation results of both observers and the intersection of those estimation results can be used to obtain the smallest intervals for the estimated state variables. The estimation result obtained with the cascaded interval observer structure and the nominal system model are shown in Fig. 6. The estimation accuracy could be improved significantly with the cascaded interval observer structure. However, the estimation of v_{TS} and v_{TL} is still conservative. We therefore investigate a second approach in the following subsection.

C. Polytopic System Model

In this approach, the time-varying part is considered using a polytopic representation of the system matrix. The matrices $\mathbf{A}$ and $\mathbf{b}$ are now time-varying, where $\mathbf{A}$ can be represented in the polytopic form

$$\mathbf{A}([\sigma(t)]) \in \left\{ \mathbf{A}(\xi) \middle| \mathbf{A}(\xi) = \sum_{\iota=1}^{3} \xi_\iota \mathbf{A}_\iota ; \sum_{\iota=1}^{3} \xi_\iota = 1 ; \xi_\iota \geq 0 \right\} . \tag{30}$$

The output matrix $\mathbf{C}$ is still a constant matrix evaluated for a chosen constant value σ_{f}, to be able to find a solution for the LMIs. Accordingly, the following system is obtained

$$\begin{aligned} \mathbf{x}_{k+1} &= \mathbf{A}_{\mathrm{d}}(\sigma_k) \cdot \mathbf{x}_k + \mathbf{b}_{\mathrm{d}}(\sigma_k) \cdot i_{\mathrm{T},k} \ , \\ \mathbf{y}_k^* &= \mathbf{C}(\sigma_{\mathrm{f}}) \cdot \mathbf{x}_k + \boldsymbol{v}_k \ . \end{aligned} \tag{31}$$

Fig. 7 shows the three vertices used to bound the dynamics matrix of system (31). Due to $\mathbf{b}_{\mathrm{d}}$ being a time-varying vector, we have to consider the supremum (infimum) of $\mathbf{T}\mathbf{b}_{\mathrm{d}}$ in (20) for the estimation of the upper (lower) bound. Here, it is important to note that the observer design is more challenging for the polytopic system approach compared to the nominal system approach, because the observer matrices have to fulfill the design conditions for every vertex of the polytope.

Remark. In this paper, the vertices for the polytopic representation were manually chosen. For more complex systems, we propose to compute the vertices using an optimization routine, for example [18]. Figs. 8 and 9 show the estimation results and the estimation errors obtained with the polytopic system approach in comparison with the estimation results and the estimation errors obtained with the nominal system approach. The polytopic representation of the system matrix leads to more accurate estimation results.

IV. Implementation Aspects

The state estimation routine is implemented in MATLAB. The system parameters of the equivalent circuit model are based on a parameter identification of an NCR 18650A battery cell in [19]. There, the parameters of the battery cell have been identified with the help of a least squares optimization which minimizes the difference between a simulated terminal voltage and a measured terminal voltage over a specific charging/discharging cycle. This parameter identification method can also be used to identify the parameters of other battery cells based on different geometries or materials. If not mentioned separately, the following simulation settings apply for all simulations presented in this paper. A sinusoidal input current as shown in Fig. 4 is used to charge and discharge the battery. The initial state and the discretization step size are chosen as $\mathbf{x}_0 = \begin{bmatrix} 0.9 & 0 & 0 & 0 \end{bmatrix}^T$ and $T_{\mathrm{d}} = 10\,\mathrm{ms}$. The magnitude of the bounded measurement noise is set to $|v| = 2.5\,\mathrm{mV}$. The measurements are generated in the simulation using uniformly distributed random numbers in the interval of $[-|v| \ ; \ |v| \ ]$. The magnitude of the process noise for the nominal discrete-time system is set to $\begin{bmatrix} 0 & 2.6 \cdot 10^{-7}\,\mathrm{V} & 1.3 \cdot 10^{-6}\,\mathrm{V} & 0 \end{bmatrix}^T$. This is based on an

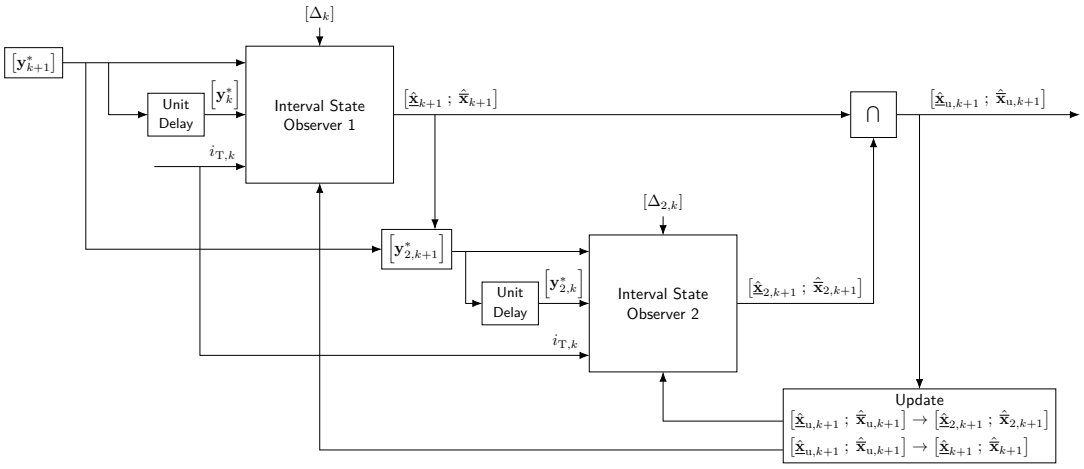

Fig. 5. Structure of the cascaded observer.

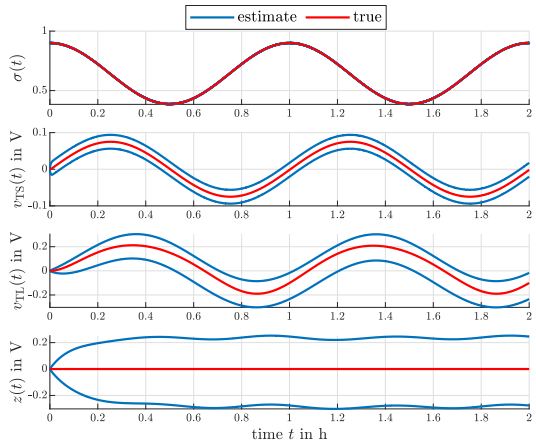

Fig. 6. Estimation result obtained with the cascaded interval observer structure.

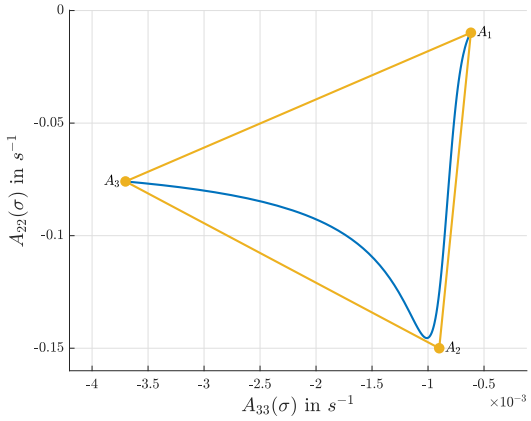

Fig. 7. Polytopic representation of the system matrix $\mathbf{A}(\sigma(t))$.

analysis of the difference between the nominal system model and the nonlinear system model for maximal and minimal input values and state variables. The fixed value σ_{f} for the SOC is set to 0.6 throughout this paper. To parameterize the observers, the LMIs are solved offline using SeDuMi and YALMIP. It is of course possible to use other LMI solvers. The scalar γ is not given beforehand, instead it is optimized within the solution of the LMIs. The cost function is set to $J = \sqrt{\gamma^2}$. In cases in which a numerical solver does not find a feasible solution for the LMIs associated with (24), iteration procedures as shown in [20] are possible.

The computational effort for evaluating the cascaded interval observer structure is approximately four times higher compared to an implementation of a Luenberger like observer for quasi-linear models with a constant gain. This is because the system model has to be evaluated for the lower and upper bounds separately and additionally it has to be evaluated for each of the two observers.

V. CONCLUSIONS

In this paper, a TNL interval observer structure has been applied for the state estimation of an uncertain time-varying quasi-linear system model of a lithium-ion battery. Two design approaches have been analyzed, which enclose the time-varying part differently. At first, a nominal system model has been considered, where the system has been divided into a time-invariant and a time-varying part. The time-varying part has been assumed to be mapped onto the process and measurement noise. This approach has lead to accurate estimation results for the first state variable, the SOC. However, the state estimation of the other state variables has been too conservative and is therefore not applicable for the identification of the dynamic behavior. To solve this issue, we have proposed a cascaded interval observer structure consisting of two TNL interval observers. The estimation results have been improved significantly with this interval observer structure. The second approach, that has been analyzed, has been based on a system model with a polytopic representation of the system matrix to consider the time-varying part. This design approach has lead to more accurate estimation results compared to the nominal design approach. The objective of this paper has been to investigate other observer designs for the state estimation of lithium-ion batteries, because in prior work an interval based Luenberger

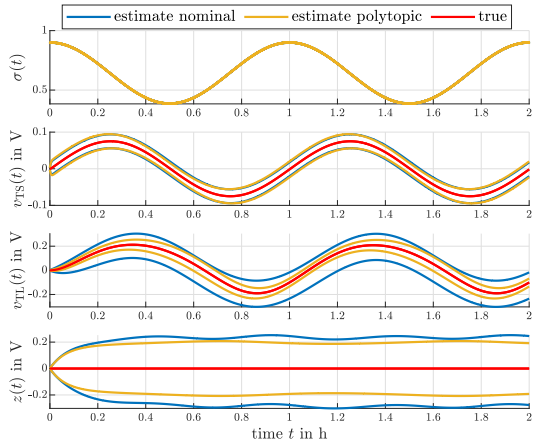

Fig. 8. Estimation result obtained with the polytopic system model.

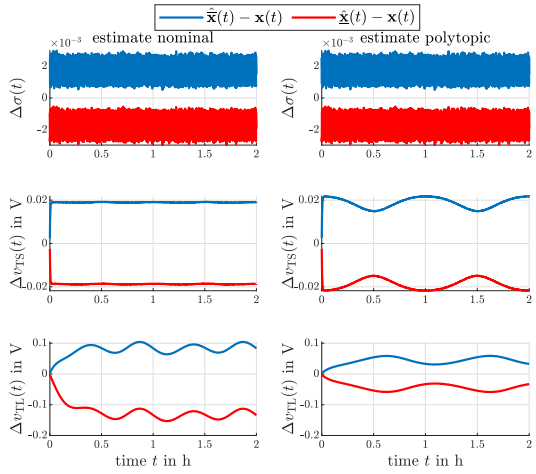

Fig. 9. Estimation errors obtained with the nominal and the polytopic system model.

like observer structure lead to an increasing estimation uncertainty over time. With both design approaches, namely the nominal system model and the polytopic system model, the estimation uncertainty does not increase over time.

For the two approaches analyzed in this paper, solving the LMIs associated with (24) with fixed output matrices $\mathbf{C}$ has been considered to include an H_∞ technique in the design process. Future work will deal with the investigation of further strategies for individually weighting the output variables to enhance the estimation accuracy of selected state variables. In cases in which the LMIs are not directly solvable, it is possible to iteratively solve the design inequalities, similar to [20]. Additionally, we will investigate, if the fixed value σ_{f} can be chosen in an optimized manner. Finally, the design of an optimal polytopic representation of the uncertain system matrix will be included in future work.

References

[1] T. Raïssi and D. Efimov, "Some recent results on the design and implementation of interval observers for uncertain systems," *at - Automatisierungstechnik*, vol. 66, no. 3, pp. 213–224, 2018.

[2] M. Lahme and A. Rauh, "Set-valued approach for the online identification of the open-circuit voltage of lithium-ion batteries," in *Proc. of the 13th Summer Workshop on Interval Methods (SWIM 2022)*. Hanover, Germany: Acta Cybernetica, 2024, in press.

[3] Z. Wang, C.-C. Lim, and Y. Shen, "Interval observer design for uncertain discrete-time linear systems," *Systems & Control Letters*, vol. 116, pp. 41–46, 2018.

[4] T. Chevet, T. N. Dinh, J. Marzat, and T. Raissi, "Interval estimation for discrete-time linear parameter-varying system with unknown inputs," in *Proc. of the 60th IEEE Conference on Decision and Control (CDC)*. Austin, Texas, USA: IEEE, 2021, pp. 4002–4007.

[5] R. Lamouchi, M. Amairi, T. Raïssi, and M. Aoun, "Active fault tolerant control using zonotopic techniques for linear parameter varying systems: Application to wind turbine system," *European Journal of Control*, vol. 67, p. 100700, 2022.

[6] J. Li, Z. Wang, W. Zhang, T. Raïssi, and Y. Shen, "Interval observer design for continuous-time linear parameter-varying systems," *Systems & Control Letters*, vol. 134, p. 104541, 2019.

[7] W. Tang, Q. Zhang, Z. Wang, and Y. Shen, "Set-membership estimation based on ellipsoid bundles for discrete-time LPV descriptor systems," *Automatica*, vol. 145, p. 110580, 2022.

[8] R. E. H. Thabet, T. Raïssi, C. Combastel, D. Efimov, and A. Zolghadri, "An effective method to interval observer design for time-varying systems," *Automatica*, vol. 50, no. 10, pp. 2677–2684, 2014.

[9] W. Tang, Z. Wang, Q. Zhang, and Y. Shen, "Set-membership estimation for linear time-varying descriptor systems," *Automatica*, vol. 115, p. 108867, 2020.

[10] Y. Ma, T. Wang, Z. Wang, and Y. Shen, "An ellipsoid-based interval estimation method for continuous-time switched systems," in *Advances in Guidance, Navigation and Control*, ser. Lecture Notes in Electrical Engineering, L. Yan, H. Duan, and Y. Deng, Eds. Singapore: Springer, 2023, vol. 845, pp. 2247–2256.

[11] S. Ahmad and H. Ahmed, "Robust intrusion detection for resilience enhancement of industrial control systems: An extended state observer approach," in *Proc. of the 2022 IEEE Texas Power and Energy Conference (TPEC)*. College Station, Texas, USA: IEEE, 2022, pp. 1–6.

[12] K. Łakomy and R. Madonski, "Cascade extended state observer for active disturbance rejection control applications under measurement noise," *ISA Transactions*, vol. 109, pp. 1–10, 2021.

[13] H. Srihi, T.-M. Guerra, A.-T. Nguyen, P. Pudlo, and A. Dequidt, "Cascade descriptor observers: Application to understanding sitting control of persons living with spinal cord injury," *Frontiers in Control Engineering*, vol. 2, 2021.

[14] F. Ramírez-Rasgado, M. Farza, O. Hernández-González, M. M'Saad, and C. M. Astorga-Zaragoza, "Observer design for a class of nonlinear system with an unknown time-delay in the output," in *2023 IEEE 11th International Conference on Systems and Control (ICSC)*. Sousse, Tunisia: IEEE, 2023, pp. 189–194.

[15] R. Galván-Guerra, L. Fridman, and J. Dávila, "High–order sliding–mode observer for linear time–varying systems with unknown inputs," *International Journal of Robust and Nonlinear Control*, vol. 27, no. 14, pp. 2338–2356, 2017.

[16] J. Huang, J. Mao, X. Dong, K. Mei, R. Madonski, and C. Zhang, "Cascaded generalized super-twisting observer design for sensorless pmsm drives," *IEEE Transactions on Circuits and Systems II: Express Briefs*, vol. 71, no. 1, pp. 331–335, 2024.

[17] M. Lahme and A. Rauh, "Combination of stochastic state estimation with online identification of the open-circuit voltage of lithium-ion batteries," in *Proc. of the 1st IFAC Workshop on Control of Complex Systems (COSY)*, vol. 40, no. 55. Bologna, Italy: IFAC-PapersOnLine, 2022, pp. 97–102.

[18] SysBrain Ltd, "Geometric bounding toolbox (GBT)," 2014, Accessed: Nov 01, 2023. [Online]. Available: http://www.sysbrain.com/gbt/gbt/index.htm

[19] J. Reuter, E. Mank, H. Aschemann, and A. Rauh, "Battery state observation and condition monitoring using online minimization," in *Proc. of the 21st International Conference on Methods and Models in Automation and Robotics (MMAR)*. Miedzyzdroje, Poland: IEEE, 2016, pp. 1223–1228.

[20] R. Dehnert, M. Damaszek, S. Lerch, A. Rauh, and B. Tibken, "Robust feedback control for discrete-time systems based on iterative LMIs with polytopic uncertainty representations subject to stochastic noise," *Frontiers in Control Engineering*, vol. 2, 2022.